

Observational evidence for a correlation between *macroturbulent* broadening and line-profile variations in OB Supergiants¹

S. Simón-Díaz

Instituto de Astrofísica de Canarias, E-38200 La Laguna, Tenerife, Spain.

Departamento de Astrofísica, Universidad de La Laguna, E-38205 La Laguna, Tenerife, Spain.

ssimon@iac.es

A. Herrero

Instituto de Astrofísica de Canarias, E-38200 La Laguna, Tenerife, Spain.

Departamento de Astrofísica, Universidad de La Laguna, E-38205 La Laguna, Tenerife, Spain.

K. Uytterhoeven

Laboratoire AIM, CEA/DSM-CNRS-Université Paris Diderot; CEA, IRFU, SAp, centre de Saclay, F-91191, Gif-sur-Yvette, France.

N. Castro

Instituto de Astrofísica de Canarias, E-38200 La Laguna, Tenerife, Spain.

Departamento de Astrofísica, Universidad de La Laguna, E-38205 La Laguna, Tenerife, Spain.

C. Aerts

Instituut voor Sterrenkunde, Katholieke Universiteit Leuven, Celestijnenlaan 200D, B-3001 Leuven, Belgium

IMAPP, Department of Astrophysics, Radboud University Nijmegen, PO Box 9010, NL-6500 GL Nijmegen, the Netherlands

and

J. Puls

Universitätssternwarte München, Scheinerstr. 1, D-81679 München, Germany

ABSTRACT

The spectra of O and B supergiants are known to be affected by a significant form of extra line broadening (usually referred to as *macroturbulence*) in addition to that produced by stellar rotation. Recent analyses of high resolution spectra have shown that the interpretation of this line broadening as a consequence of large scale turbulent motions would imply highly supersonic velocity fields in photospheric regions, making this scenario quite improbable. Stellar oscillations have been proposed as a likely alternative explanation. As part of a long term observational project, we are investigating the macroturbulent broadening in O and B supergiants and its possible connection with spectroscopic variability phenomena and stellar oscillations. In this letter, we present the first encouraging results of our project, namely firm observational evidence for a strong correlation between the extra broadening and photospheric line-profile variations in a sample of 13 supergiants with spectral types ranging from O9.5 to B8.

Subject headings: stars: early-type — stars: atmospheres — stars: oscillations — stars: rotation — supergiants

1. Introduction

The presence of an important extra line broadening mechanism (in addition to the rotational broadening and usually called *macroturbulence*) affecting the spectra of O and B supergiants (Sgs) was initially suggested by the deficit of narrow lined objects among these types of stars (e.g. Slettebak 1956; Conti & Ebbets 1977; Howarth et al. 1997). The advent of high-quality spectra permitted confirmation that rotational broadening alone is insufficient to fit the line profiles in many objects, and to investigate the possible disentangling of both broadening contributions (see e.g. Ryans et al. 2002; Simón-Díaz & Herrero 2007). These studies definitely showed that the effect of macroturbulence is dominant in the profiles of metal lines in early B Sgs.

Although it was named macroturbulence at some point, the interpretation of this extra broadening as the effect of turbulent motion is quite improbable. The effect is present in photospheric lines and affects the whole profile, even wavelengths close to the continuum. Therefore, whatever is producing the extra broadening has to be deeply rooted in the stellar photosphere (and possibly deeper), in layers where we do not expect any significant velocity field in these stars.

If interpreted as turbulent motion, macroturbulence would represent *highly supersonic* velocities in many cases (see Figure 1). This interpretation is incompatible with the previous statement.

One physical mechanism suggested as the origin of this extra broadening relates to oscillations. Many OB Sgs are known to show photometric and spectroscopic variability. Based on this, Lucy (1976) postulated that this variability might be a pulsation phenomenon, and macroturbulence may be identified with the surface motions generated by the superposition of numerous non-radial oscillations. More recently, Aerts et al. (2009) computed time series of line profiles for evolved massive stars broadened by rotation and thousands of low amplitude non-radial gravity mode oscillations and showed that the resulting profiles could

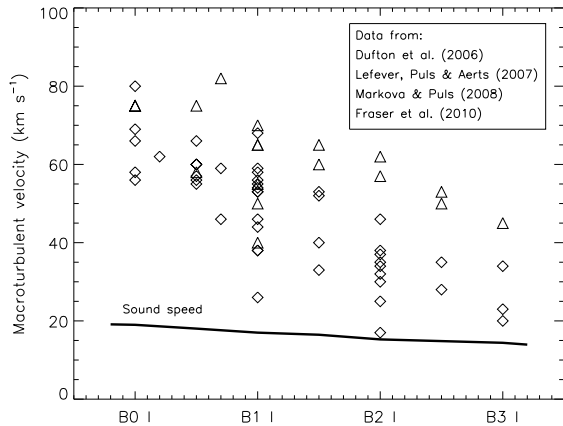


Fig. 1.— Macroturbulent velocities for B Sgs with spectral types B0-B3, measured in recent studies. Two different symbols are used depending on the type of definition assumed for the macroturbulent profile. Diamonds: isotropic Gaussian (Dufton et al. 2006; Fraser et al. 2010); triangles: radial-tangential definition (Lefever et al. 2007; Markova et al. 2008). Characteristic values for the sound speed in the photospheres of these types of stars are also indicated as a solid line.

mimic the observed ones. In their paper, Aerts et al. (2009) considered the amplitudes of the pulsation modes to be sufficiently low to allow a linear superposition of mode velocities to derive the overall pulsational velocity eigenvector, i.e., non-linear mode coupling or other nonlinear effects were ignored. We refer the reader to Sect. 2.1 in Aerts et al. (2009) for a detailed description of the simulations, and a discussion about how the collective effect of low amplitude non-radial gravity modes can produce the inferred supersonic level of macroturbulent broadening when the oscillations are ignored in the interpretation of spectral lines. Stellar oscillations are a plausible explanation for the extra broadening in O and B Sgs, but so far there is no direct observational evidence confirming this hypothesis.

Two years ago we began an observational project aimed at investigating the macroturbulent broadening in O and B Sgs, and its possible connection with spectroscopic variability phenomena and stellar oscillations. In this letter, we present the first encouraging results, showing observational evidence for a strong correlation between

¹Based on observations made with the Nordic Optical Telescope, operated on the island of La Palma jointly by Denmark, Finland, Iceland, Norway, and Sweden, in the Spanish Observatorio del Roque de los Muchachos of the Instituto de Astrofísica de Canarias.

this extra broadening and photospheric line profile variations in a sample of 13 Sgs with spectral types ranging from O9 to B8.

The letter is structured as follows: the sample of stars and the spectroscopic observations used for this study are presented in Sect. 2; we characterize the line-broadening and the line-profile variations of photospheric lines in Sects. 3 and 4, respectively; a connection between the extra broadening and line profile variations is presented in Sect. 5. Finally, we discuss the possible relation to stellar pulsations in Sect. 6.

2. Observational data set

We obtained time series spectra of a selected sample of 11 bright late-O and early-B Sgs during two observing runs (2008/11/05-08, 2009/11/09-12) with the FIES cross-dispersed high resolution echelle spectrograph on the 2.5m Nordic Optical Telescope at Roque de los Muchachos Observatory on La Palma (Canary Islands, Spain). We used FIES in the medium resolution mode ($R=46000$, $\delta\lambda=0.03$ Å/pix). The sample was complemented with two OB dwarfs and two late B Sgs. The exposure times were chosen so as to reach at least $SNR=200$ (measured in the range 4500–4600 Å). The list of observed stars, along with their spectral classification, number of spectra obtained for each target, timespan of the corresponding time-series, and observing run in which they were observed are indicated in the first columns of Table 1. Note that four of these stars were observed in both campaigns.

The spectra were reduced with the FIEStool² package in advanced mode. A proper set of bias, flat and arc frames obtained each night was used to this aim. The FIEStool pipeline provided wavelength-calibrated, blaze-corrected, order-merged spectra of high quality. Next, the barycentric correction was performed. We used the interstellar Na ID doublet at 5890 Å to check the accuracy in this correction, and found an agreement in the line doublet position for all the time series spectra of each star better than 0.5 km s⁻¹.

Once the lines of interest for this study were identified, a local normalization of selected regions

of the spectra was performed. For each line, the local continuum used for the normalization was calculated from a linear fit between points inside two continuum regions adjacent to the line. The same continuum windows (selected manually in the average spectrum) were used for all the spectra of a given star.

3. Characterization of the line broadening in photospheric lines

Several types of broadening mechanisms are traditionally considered to produce the final observed line profiles of photospheric metal lines in massive stars: instrumental, natural, thermal, microturbulent, macroturbulent and rotational broadening. In the case of high resolution³ spectra of late-O and early B Sgs, rotational and macroturbulent contributions dominate.

We used the Fourier transform technique (Gray 1976; see also Simón-Díaz & Herrero, 2007 for a recent application to the spectra of O and B stars) to disentangle the contributions from rotational and macroturbulent broadening. The results of the analysis are presented in Table 1. We performed the analysis for each of the time series spectra, obtaining $v \sin i$ as indicated by the first zero of the Fourier transform. The range and median of derived $v \sin i$ values are indicated in columns 6 and 7 of Table 1. Note that the dispersion in the obtained $v \sin i$ values is between 10% and 30%, depending on the star. Whether this dispersion is real or an effect of noise is not clear from this dataset. As outlined by Simón-Díaz & Herrero (2007), the correct identification of the first zero is complicated in cases of low SNR and for a large extra broadening contribution. This will be explored in more detail in a future investigation.

Next, we applied a goodness-of-fit method (viz. Ryans et al. 2002) to quantify the contribution of the extra broadening in each spectrum from the time series. We considered as free parameters the equivalent width, the radial velocity, $v \sin i$, and the parameter defining the extra broadening. We allowed $v \sin i$ to vary in the fitting process in order to compare with results from the FT anal-

²<http://www.not.iac.es/instruments/fies/fiestool/FIEStool.html>

³ The instrumental broadening contribution can be minimized by using high resolution spectra. In our FIES@NOT data set ($R=46000$) the instrumental Gaussian profile has a FWHM ~ 6.5 km s⁻¹.

Table 1: Columns 1–5: Targets, spectral classification, observing campaign, timespan of the observations, and number of spectra. Columns 6–11: Line-broadening and LPVs characterization in the Si III 4567 or O III 5592 lines for our stellar sample. LPVs characterized with the peak-to-peak amplitudes of the first and third moments of the lines. ΔT in days; $v \sin i$, Θ_{RT} , $\langle v \rangle_{\text{pp}}$, and $\langle v^3 \rangle_{\text{pp}}^{1/3}$ in km s^{-1} . Uncertainties in $\langle v \rangle_{\text{pp}}$, and $\langle v^3 \rangle_{\text{pp}}^{1/3}$ are ~ 0.10 - 0.30 and ~ 0.4 - 1.2 km s^{-1} , respectively

Star	SpT & LC	Run	ΔT	#	$v \sin i$ (FT)		χ^2 fitting		LPVs	
					Range	Median	$\langle v \sin i \rangle$	$\langle \Theta_{\text{RT}} \rangle$	$\langle v \rangle_{\text{pp}}$	$\langle v^3 \rangle_{\text{pp}}^{1/3}$
HD 207198	O9 Ib-II	FI09	3.14	14	59–64	62±2	50±2	100±0	3.41	26.9
HD 209975	O9.5 Iab	FI08	3.04	21	56–62	59±2	50±6	95±5	10.13	46.3
		FI09	3.18	18	52–58	57±2	51±4	100±5	11.65	45.4
HD 37742	O9.7 Ib	FI09	3.19	30	90–140	117±10	115±15	117±13	12.01	62.8
HD 204172	B0 Ib	FI09	3.14	14	38–68	58±11	58±6	85±5	11.80	44.0
HD 37128	B0 Ia	FI08	3.01	60	45–64	55±9	57±8	90±6	12.30	43.0
		FI09	3.18	28	32–60	49±8	54±9	90±9	13.02	46.5
HD 38771	B0.5 Ia	FI08	2.99	48	42–57	50±6	48±5	90±6	9.38	36.6
		FI09	3.17	25	30–55	48±8	52±7	90±5	10.56	39.1
HD 2905	BC0.7 Ia	FI08	3.07	30	44–58	53±5	51±6	90±3	10.07	39.8
		FI09	3.29	28	33–65	49±11	61±2	85±5	11.49	39.6
HD 24398	B1 Iab:	FI09	3.19	34	27–43	34±5	38±2	65±0	3.15	25.7
HD 190603	B1.5 Ia ⁺	FI08	1.96	17	30–47	46±5	49±4	55±3	2.18	24.6
HD 14818	B2 Ia	FI08	3.00	16	32–47	41±6	41±5	70±3	7.84	37.1
HD 206165	B2 Ib	FI09	3.14	16	29–41	38±2	38±2	60±0	5.63	28.2
HD 191243	B5 Ib	FI09	2.10	9	15–25	18±3	18±2	30±0	1.36	13.4
HD 34085	B8 Iab:	FI09	3.08	21	14–33	23±4	29±4	35±5	6.18	19.8
HD 214680	O9 V	FI08	3.12	31	13–23	18±3	16±2	40±5	2.12	17.4
HD 37042	B0.5 V	FI08	2.92	20	32–34	33±1	33±0	15±5	0.84	10.4

ysis. Two possibilities for the characterization of the extra broadening were considered: an isotropic Gaussian profile, and a Gaussian radial–tangential one (Θ_{RT} , see Gray 1976). In the latter, we assumed that the radial and tangential components provide equal contributions to the final profile. The analysis using an isotropic Gaussian profile for the macroturbulent broadening resulted in (a) a large dispersion in the $v \sin i$ values obtained from the various spectra in each time series; (b) systematically lower $v \sin i$ values than those determined through the FT method (a factor of 0.5 in many cases, sometimes even “zero” rotation) for all stars with dominant extra broadening. On the other hand, when assuming a Gaussian radial–tangential profile, we found that (a) the dispersion in the $v \sin i$ and Θ_{RT} values was rather low; (b) differences between the $v \sin i$ values obtained from the goodness-of-fit method and using the FT technique are $\leq \pm 20\%$. We thus conclude that a Gaussian radial–tangential profile is better suited to characterizing the extra line broadening than an isotropic Gaussian profile.⁴ The corresponding

mean and standard deviation for $v \sin i$ and Θ_{RT} as obtained from the χ^2 fit are indicated in columns 8 and 9 in Table 1. Note the good agreement in the derived values for the four stars observed in both 2008 and 2009.

Similarly to previous studies (e.g. Dufton et al. 2006; Lefever et al. 2007; Markova et al. 2008; Fraser et al. 2010), we found that the size of the extra broadening is generally larger than the rotational contribution in all the Sgs. This is not the case for the B0.5 V star HD 37042, where the total broadening is mainly produced by the effect of the stellar rotation (note, however, that a certain extra broadening is also needed in this case). The other dwarf star, HD 214680, is a special case, since it has very low $v \sin i$. For such a low $v \sin i$ values, microturbulence produces a significant contribution to the total broadening, which then is included in the measured extra broadening. Note that this argument may also explain the extra broadening needed for HD 37042 (and the other two late-B Sgs with low $v \sin i$).

subtle.

⁴We also found that the former generally produces a better final fit to the observed profiles, though the differences are

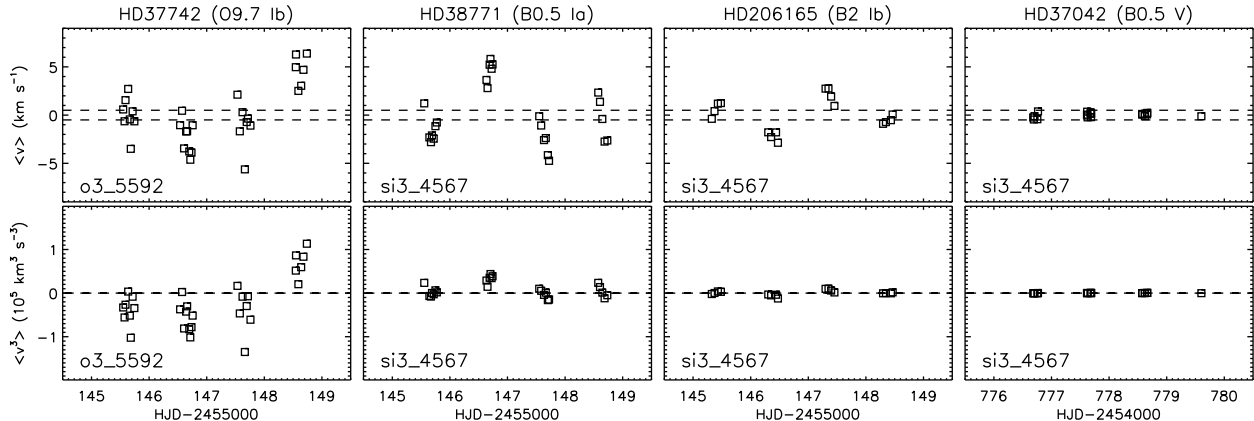


Fig. 2.— Representative examples for the variation of the first moment (radial velocity placed at average zero) and third moment (skewness of the line) for some of the stars in the studied sample derived from the Si III 4567 or O III 5592 line profiles. Horizontal lines in upper plots show the accuracy in radial velocity associated with the instrumental setting used for FIES@NOT.

4. Characterization of line profile variations in photospheric lines

In agreement with earlier studies of spectroscopic variability in O and B Sgs (e.g. Ebbets 1982; Howarth et al. 1993; Fullerton, Gies, & Bolton 1996; Prinja et al. 1996, 2004, 2006; Morel et al. 2004; Kaufer et al. 2006; Markova et al. 2005, 2008), we found clear signatures of line profile variations (LPVs) for all the Sgs considered in our sample. To investigate these LPVs quantitatively we computed the first, $\langle v \rangle$, and third, $\langle v^3 \rangle$, normalized velocity moments (for definitions, see, e.g., Aerts et al. 2010a) from the Si III 4567 or O III 5592 lines with FAMIAS⁵ (Zima 2008). These moments are related to the centroid velocity and the skewness of the line profile, respectively, and are well suited for deciding whether an observed line profile is subject to time-dependent line asymmetry (note that their values are zero for purely symmetric profiles).

Four representative examples of the temporal behavior of the first and third velocity moments are presented in Fig. 2. The associated uncertainties (not included in the plot) are ~ 0.1 – 0.4 km s^{-1} , and ~ 1000 – $4000 \text{ km}^3 \text{ s}^{-3}$, respectively. In the case of the dwarf star HD 37042,

the $\langle v \rangle$ values are fairly constant and close to zero. The maximum dispersion in velocity for this star is $\sim 1 \text{ km s}^{-1}$, of the order of the accuracy associated with the instrumental setting used for the FIES@NOT observations (indicated as dashed horizontal lines). All the other stars in Figure 2 show $\langle v \rangle$ variations above this significance level, with maximum peak-to-peak amplitudes reaching ~ 10 – 12 km s^{-1} in some of the cases. The minimum variations are found for HD 214680 (the other luminosity class V object considered in this study), HD 191243 (B5 Ib) and HD 190603 (B1.5 Ia⁺), with maximum amplitudes slightly larger than the significance level. Curiously, the star HD 190603, expected to be an extreme object from its spectral classification, is one of the cases with smaller variations. We indicate in Table 1 (columns 10 and 11) the peak-to-peak amplitude of the first and third moment variations measured for each of the considered targets.

5. The “macroturbulence”-LPV connection

We investigate the possible connection between macroturbulent broadening and LPVs in our sample of stars. Such a connection should appear in case macroturbulent broadening is produced by any time-dependent physical phenomena (e.g. non-radial oscillations, see Aerts et al. 2009). In Fig. 3 (upper panels), we plot the average size of

⁵A software package developed in the framework of the FP6 European Coordination Action HELAS (<http://www.helas-eu.org/>).

the macroturbulent broadening, $\langle\Theta_{\text{RT}}\rangle$, versus the peak-to-peak amplitude of $\langle v \rangle$ and $\langle v^3 \rangle$ variations for each of the stars studied. Results from the four stars observed in both campaigns are connected with solid lines. A clear positive correlation is present in both cases. To our knowledge, this is the *first clear observational evidence for a connection between extra broadening and LPVs in B and late O Sgs*. Particularly remarkable is the $\Theta_{\text{RT}} - \langle v^3 \rangle$ correlation: the larger the extra broadening, the more asymmetric line profiles can be found in the time series. Note that this does not mean that lines with a significant macroturbulence contribution are always asymmetric since $\langle v^3 \rangle$ oscillates between positive and negative values over time.

We also present in Fig. 3 (bottom panels) similar plots with data from Table 1 in Aerts et al. (2009), based on simulations of v line profiles broadened by rotation and by hundreds of low amplitude non-radial gravity mode pulsations. These simulations consider various combinations of the inclination angle (i), the projected rotational velocity ($v \sin i$), and the intrinsic amplitude of the modes denoted by a (see Aerts et al. 2009, for a definition). We present the maximum values of v_{mac} obtained for each set of simulated profiles. Similar trends for v_{mac} as in Fig. 3 are found using average or minimum values for the macroturbulence parameter, but with a different (smaller) scale in the y-axis.

The simulations lead to clear trends which are compatible with spectroscopic observations.

6. Is macroturbulent broadening in OB-Sgs caused by pulsations?

Non-radial oscillations have been often suggested as the origin of LPVs and photospheric lines in OB Sgs, as well as the driver of large scale wind structures (see references in Sect. 4); however, a firm confirmation (by means of a rigorous seismic analysis) has not been achieved yet. From a theoretical point of view, g-mode oscillations were not initially expected in B Sgs because the radiative damping in the core was suspected as being too strong. Saio et al. (2006) detected simultaneous p- and g-modes in HD 163899 (B2 Ib/II) using data from the MOST satellite. These authors also computed new models showing that g-modes can be excited in massive post-main sequence stars, as

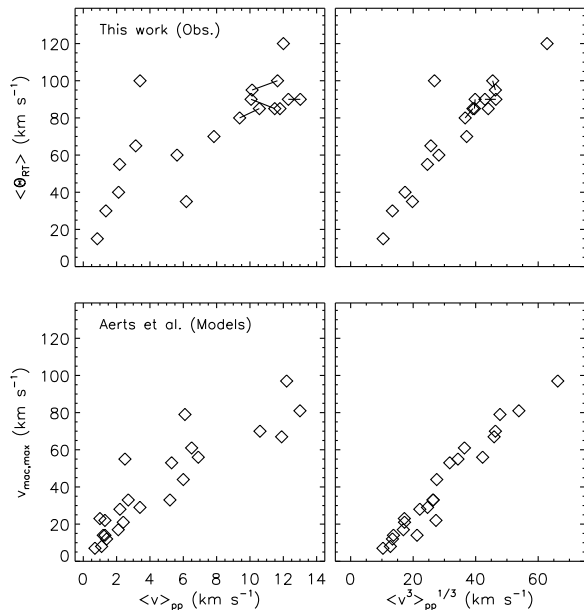


Fig. 3.— (Top) Empirical relations between the average size of the macroturbulent broadening ($\langle\Theta_{\text{RT}}\rangle$) and the peak-to-peak amplitude of the first and third moments of the line-profile. (Bottom) Similar relations are found from the simulations by Aerts et al. (2009).

the g-modes are reflected at the convective zone associated with the H-burning shell. Lefever et al. (2007) presented observational evidence of g-mode instabilities in a sample of photometrically variable B Sgs from the location of the stars in the $(\log g, \log T_{\text{eff}})$ -diagram.

These results, along with our observational confirmation of a tight connection between macroturbulence and parameters describing observed LPVs render stellar oscillations the most probable physical origin of macroturbulent broadening in B Sgs; however, it is too premature to consider them as the only physical phenomenon to explain the unknown broadening.

Recent studies of high resolution spectra of OB stars indicate that the appearance of a significant macroturbulent broadening contribution is not only limited to B Sgs but occurs also in O stars of all luminosity classes (Simón-Díaz et al. 2010; Markova et al. 2010) as well as in main-sequence B-type pulsators (e.g. Morel et al. 2006). Moreover, with the recent discovery of a strange-

mode oscillation in the B6Ia supergiant HD 46005 (Aerts et al. 2010b) and of stochastic oscillations in the O8V star HD 46149 (Degroote et al. 2010) and the β Cephei star V1449 Aql (Belkacem et al. 2009) from high-precision space photometry, observational evidence of atmosphere phenomena due to oscillations, which *must* cause some level of pulsational broadening, is growing.

Future investigations of the correlation between LPVs and macroturbulence, and its connection to stellar oscillations in the whole realm of massive stars, will be key to establishing the role played by the different physical processes contributing to the spectral line formation in these types of stars. Different models including various combinations of pulsational, rotational and wind effects should be considered, keeping in mind that an appropriate physical mechanism must be able to explain the observed correlation presented in this study.

Financial support from the Spanish Ministerio de Ciencia e Innovación under the project AYA2008-06166-C03-01 is acknowledged. This work has also been partially funded by the Spanish MICINN under the Consolider-Ingenio 2010 Program grant CSD2006-00070: First Science with the GTC (<http://www.iac.es/consolider-ingenio-gtc>). The research leading to these results has also received funding from the European Research Council under the European Community's Seventh Framework Programme (FP7/2007–2013)/ERC grant agreement n°227224 (PROSPERITY).

REFERENCES

- Aerts, C., Puls, J., Godart, M., & Dupret, M.-A. 2009, *A&A*, 508, 409
- Aerts, C., Christensen-Dalsgaard, J., & Kurtz, D. W. 2010a, *Asteroseismology* (Springer)
- Aerts, C., Lefever, K., Baglin, A., Degroote, P., Oreiro, R., Vučković, M., Smolders, K., Acke, B., Verhoelst, T., Desmet, M., Godart, M., Noels, A., Dupret, M.-A., Auvergne, M., Baudin, F., Catala, C., Michel, E., Samadi, R. 2010b, *A&A*, 513, L11
- Belkacem, K., et al. 2009, *Science*, 324, 1540
- Conti, P. S., & Ebbets, D. 1977, *ApJ*, 213, 438
- Degroote, P., Briquet, M., Auvergne, M., Simón-Díaz, S., Aerts, C., Noels, A., Rainer, M., Hareter, M., Poretti, E., Mahy, L., Oreiro, R., Vuckovic, M., Smolders, K., Baglin, A., Baudin, F., Catala, C., Michel, E., Samadi, R. 2010, *A&A*, in press (arXiv:1006.3139)
- Dufton, P. L., Ryans, R. S. I., Simón-Díaz, S., Trundle, C., & Lennon, D. J. 2006, *A&A*, 451, 603
- Ebbets D. 1982, *ApJS*, 48, 399
- Fraser, M., Dufton, P. L., Hunter, I., & Ryans, R. S. I. 2010, *MNRAS*, 404, 1306
- Fullerton A. W., Gies D. R., & Bolton C. T. 1996, *ApJS*, 103, 475
- Gray, D. F. 1976, *The Observations and Analysis of Stellar Photospheres* (1st ed.; New York: Wiley)
- Howarth I. D., et al. 1993, *ApJ*, 417, 338
- Howarth, I. D., Siebert, K. W., Hussain, G. A. J., & Prinja, R. K. 1997, *MNRAS*, 284, 265
- Kaufer A., Stahl O., Prinja R. K., & Witherick D. 2006, *A&A*, 447, 325
- Lefever, K., Puls, J., & Aerts, C. 2007, *A&A*, 463, 1093
- Lucy, L. B. 1976, *ApJ*, 206, 499
- Markova N., Puls J., Scuderi S., & Markov H. 2005, *A&A*, 440, 1133
- Markova N., Prinja R. K., Markov H., Kolka I., Morrison N., Percy J., & Adelman S. 2008, *A&A*, 487, 211
- Markova, N., et al. 2010, in preparation
- Morel, T., Marchenko, S. V., Pati, A. K., Kuppuswamy, K., Carini, M. T., Wood, E., & Zimmerman, R. 2004, *MNRAS*, 351, 552
- Morel, T., Butler, K., Aerts, C., Neiner, C., & Briquet, M. 2006, *A&A*, 457, 651
- Prinja R. K., Fullerton A. W., & Crowther P. A. 1996, *A&A*, 311, 264

- Prinja, R. K., Rivinius, T., Stahl, O., Kaufer, A.,
Foing, B. H., Cami, J., & Orlando, S. 2004,
A&A, 418, 727
- Prinja R. K., Markova N., Scuderi S., & Markov
H. 2006, A&A, 457, 987
- Ryans, R. S. I., Dufton, P. L., Rolleston, W. R. J.,
Lennon, D. J., Keenan, F. P., Smoker, J. V., &
Lambert, D. L. 2002, MNRAS, 336, 577
- Saio, H., et al. 2006, ApJ, 650, 1111
- Simón-Díaz, S., & Herrero, A. 2007, A&A, 468,
1063
- Simón-Díaz, S., et al. 2010, in preparation
- Slettebak, A. 1956, ApJ, 124, 173
- Zima W. 2008, CoAst, 155, 17